First-principles calculations of Cu adsorption on an H-terminated Si surface

A. S. Foster,[1,*] M. A. Gosálvez,[2] T. Hynninen,[1] R. M. Nieminen,[1] and K. Sato[2]
[1]*Laboratory of Physics, Helsinki University of Technology, P.O. Box 1100, 02015 HUT, Finland*
[2]*Department of Micro-Nano Systems Engineering, Nagoya University, Nagoya 464-8603, Japan*
(Received 20 March 2007; revised manuscript received 21 May 2007; published 9 August 2007)

In this study, we use first-principles simulations to study the adsorption of copper onto H-terminated and partially OH-terminated silicon surfaces. We show that, in contrast to previous studies, copper adsorbs strongly to the H-terminated silicon surface and that the adsorption energy is significantly dependent on the local bonding environment. The addition of a hydroxide group increases the average adsorption energy while reducing the range of adsorption energies due to the strong interaction between copper and oxygen. Our results predict that copper will generally prefer to adsorb at dihydride sites on the surface, agreeing with experimental studies of copper nucleation. The adsorption energy hierarchy predicted by the calculations strongly supports the suggestion that copper acts as a micromask in wet chemical etching, blocking reactive sites.

DOI: 10.1103/PhysRevB.76.075315 PACS number(s): 68.43.−h, 81.65.Cf, 73.20.Hb

I. INTRODUCTION

The reduction in scale of silicon-based microelectronics devices has increased their sensitivity to contamination, and controlling impurities has become a critical problem. Amongst the most common metal impurities, copper has been shown to be much more damaging to electrical properties than, for example, aluminium, iron, or nickel.[1,2] Copper is introduced as a contaminant in several ways, depending on the processing route. Most recently, the adoption of copper as the interconnect material in ultralarge scale integrated devices means that copper can diffuse directly into and through silicon.[3] A more longstanding source of copper contamination is via chemical processing of silicon, particularly through cleaning of the silicon wafer with acid.[4] Silicon wafer cleaning is an unavoidable part of device preparation, necessary to remove silicon oxide before crucial process steps, such as gate oxidation and dopant diffusion, and copper spontaneously deposits to the surface from the cleaning solution (usually HF).[5] Similarly, solutions used to etch silicon itself contain significant metal impurities, including copper, and the role of copper in etched morphologies is a significant issue in micro- and nanoelectromechanical-system fabrications.[6] Due to its high diffusion[3] and reactivity in silicon, copper has also attracted interest in the design of nanostructured surfaces and deposition of nanowires,[7–10] in analogy with the surface templating demonstrated with Ga.[11]

The deposition and growth of copper on the clean silicon surface have been experimentally studied by a variety of techniques, especially scanning tunneling microscopy.[10,12–17] Despite the large number of experimental studies, most of the previous theoretical studies, for example,[18–21] have focused on the properties of copper impurities in bulk silicon, and very few have approached copper adsorption on the surface. Furthermore, in many applications, the surface is hydrogen-terminated due to the cleaning process, and studies of the interaction of copper and silicon in the presence of hydrogen have been even more limited.[10,20,22,23] A comparative study of copper deposition on the clean and hydrogen-terminated silicon (111) surface showed that the growth modes are quite similar at room temperature, but that at higher temperatures (570–770 K) copper is much more mobile on the hydrogen-terminated surface.[22] Theoretical predictions support the mobility of copper on a hydrogen-terminated surface,[23] but the very low calculated adsorption energies are difficult to reconcile with etching experiments.[6]

According to wet etching experiments in alkaline solutions,[24–26] Cu has a dramatic impact on the etch rate, the surface morphology, and the surface roughness of (110) and (100). During KOH etching, the surface is mostly H terminated,[27,28] although it includes a small fraction of OH terminations,[29] whose number is expected to increase with increasing KOH concentration. As compared to other metal impurities, copper seems to have a particular preference to adsorb on the H-terminated surface during etching, presumably acting as a blocking agent ("micromask") once it has been attached, locally reducing the etching probability.[6] As an example, the addition of copper to the etching solution directly increases the number of hillocks that are formed on both (100) and (110) silicon surfaces.

In this work, we use first-principles calculations to systematically study the adsorption of copper onto the hydrogen-terminated silicon surface, including also the effects of local hydroxyl terminations of relevance for wet etching studies, and compare our results to experiments with direct links to important applications in silicon processing technology. As far as we are aware, this is the first theoretical work which addresses the adsorption of copper on a hydrogen-terminated surface with and without the effects of local hydroxyl terminations.

II. METHODS

A. Calculation methodology

The calculations were performed using the linear combination of atomic orbital basis SIESTA code,[30,31] implementing the density functional theory within the generalized gradient approximation. We use the functional of Perdew, Burke, and Ernzerhof.[32] Core electrons are represented by norm-conserving pseudopotentials using the Troullier-Martins parametrization and including scalar relativistic corrections.

 ©2007 The American Physical Society

The pseudopotential for the silicon atom was generated in the electron configuration [Ne]$3s^2 3p^2$, for oxygen in [$1s^2$]$2s^2 2p^4$, for copper in [Ar]$4s^1 3d^{10}$, and for hydrogen in $1s^1$, with the square brackets denoting the core electron configurations. After extensive testing of different basis sets, we used double zeta with a single shell of polarization orbitals for Si and H, double zeta with two shells of polarization orbitals for oxygen, and triple zeta with two shells of polarization orbitals for copper. The energy shift used (25 meV) corresponded to maximum cutoffs of 8.5 Bohr radii (a_0), $5.3a_0$, $6.5a_0$, and $8.7a_0$ for Si, O, H, and Cu, respectively. This basis set is significantly better than that considered qualitatively equivalent to fully converged plane wave calculations.[21]

The system's properties were converged with respect to k points [apart from for bulk copper, a $(2\times 2\times 1)$ Monkhorst-Pack[33] mesh was sufficient for all systems] and mesh (cutoff 150 Ry). Adsorption energies were calculated with respect to the isolated surface and atom, and include counterpoise corrections[34] for basis set superposition errors. Initial calculations on bulk silicon and copper and silicon surfaces using this setup showed good agreement with experiment and previous calculations.

For etching and acid cleaning applications, copper impurities are originally present as cations in solution, e.g., $Cu(NO_3)_2$. However, the copper ions are reduced near the surface and will adsorb in the neutral state.[24,26] For other applications, copper is usually present as a metal, but in any case, since silicon is usually doped for microelectronics purposes, it can be considered as an unlimited reservoir of electrons, and the adsorption of an initially neutral copper atom is physically valid.

B. System setup

All the structures investigated in this work are initially based on the H-terminated silicon (111) surface, which we model by a periodic two-dimensional slab with the base also terminated by hydrogen to saturate dangling bonds. We tested the dependence of our results on the number of surface layers and found that generally three or four layers of silicon converged the properties of the surface. The base hydrogens and lowest layer of silicon were kept frozen to model the bulk structure, and all other atoms were allowed to relax freely until atomic forces were less than 0.02 eV/Å. Since, in this study, we are interested in the interaction of copper with realistic surfaces, most calculations were performed on stepped or kinked Si(111) surfaces so that we could sample a large variety of adsorption sites. The most common surface features are monohydride steps (see Fig. 1), horizontal dihydride steps (see Fig. 2), vertical dihydride steps (see Fig. 3), kinks on horizontal dihydride steps [see Fig. 4(a)], and kinks on monohydride steps [see Fig. 4(b)]—a detailed study of the different surface features can be found in Ref. 6. In total, we found 17 stable adsorption sites amongst the different surface configurations, although we considered many more sites initially. The sites most important for understanding the adsorption behavior of copper on the surface are labelled throughout Figs. 1–4, and these will be discussed in more detail in Sec. III. The site labels follow the conventions established in Ref. 6.

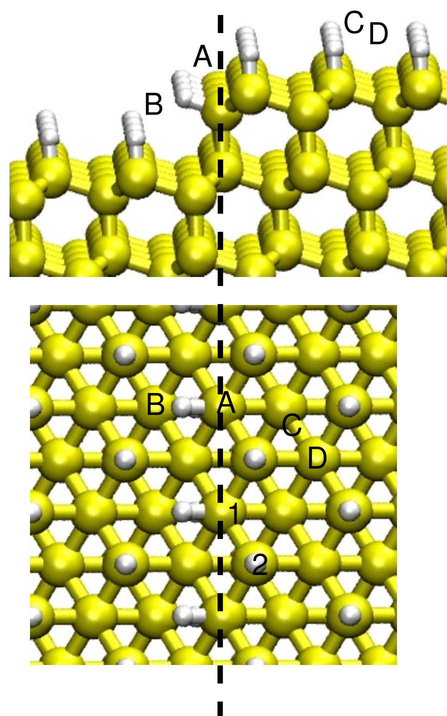

FIG. 1. (Color online) Side and overhead views of the atomic structure of a monohydride step. Silicon is represented by large yellow (large light gray) spheres, and hydrogen by small white spheres.

Since the calculations are periodic, we paid particular attention to the size of the unit cell used to represent each

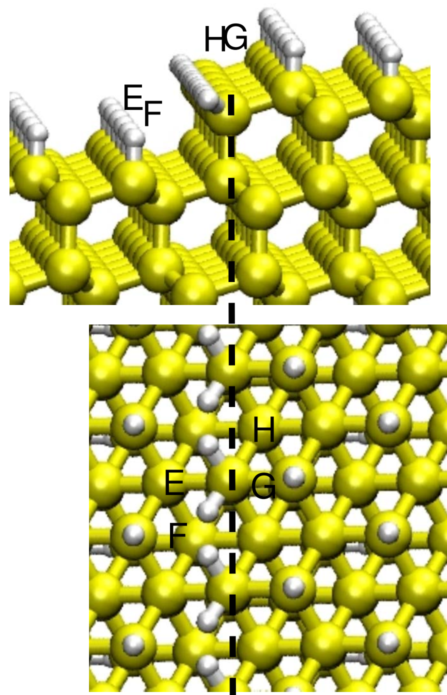

FIG. 2. (Color online) Side and overhead views of the atomic structure of a horizontal dihydride step. Colors as in Fig. 1.

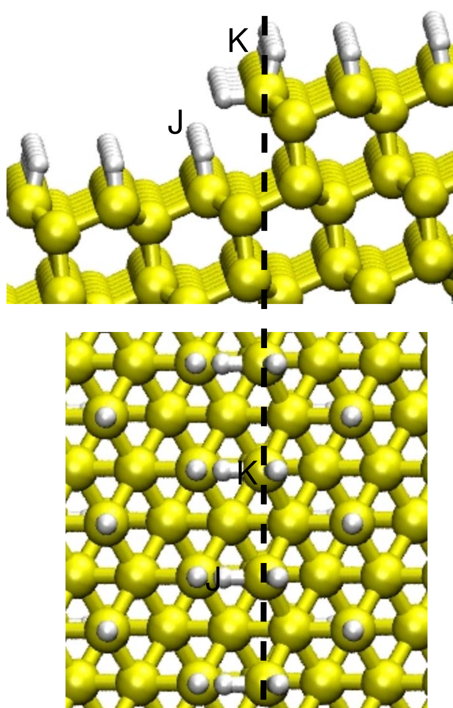

FIG. 3. (Color online) Side and overhead views of the atomic structure of a vertical dihydride step. Colors as in Fig. 1.

surface configuration. As the interaction ranges are determined by cutoffs, it is very straightforward to establish whether *fake* interactions have been introduced. For example, the vacuum gap in the z direction was large enough to avoid interactions between surfaces. Furthermore, in every case, the distance in the x direction (from left to right in

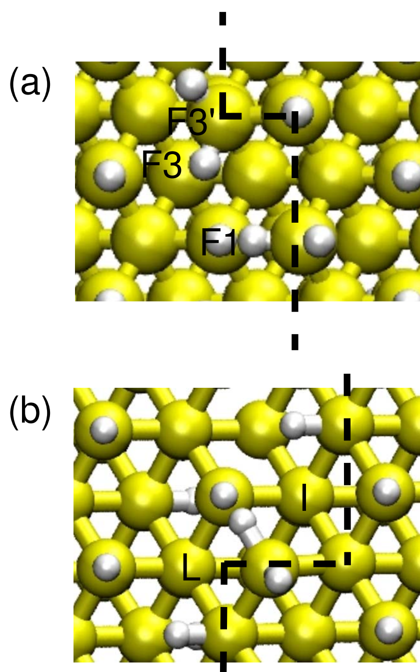

FIG. 4. (Color online) Overhead views of the atomic structure of (a) a kink in a horizontal dihydride step and (b) a kink in a monohydride step. Colors as in Fig. 1.

TABLE I. Copper adsorption energies on various sites on the silicon (111) surface.

System	E (eV)
A	−0.55
B	−0.89
C	−0.77
D	−1.17
E	−1.01
F	−1.43
F1	−1.44
F3	−1.34
F3′	−0.43
G	−0.63
H	−1.39
I	−1.34
J	−1.10
K	−0.50
L	−1.01
M	−0.65
N	−1.27
A+OH	−1.38
C+OH	−0.98
D+OH	−1.14
E+OH	−1.20
F1+OH	−1.34
F3+OH	−1.06

Fig. 1) between step edges was over $18a_0$ (usually much larger), far beyond the interaction cutoff, and the step edge interactions do not play a role in the adsorption. However, for some systems, the effective distances between defected sites in the y direction (along the dashed line in Fig. 1) was smaller due to extensive relaxations of atoms neighboring the *action* site. In these cases, we doubled the size of the unit cell in the y direction, but found no significant difference in geometry or configuration energies.

III. RESULTS

A. Adsorption on the H-terminated surface

1. Adsorption energies

The adsorption energies for all the stable sites considered in this study are shown in Table I. Firstly, we consider adsorption on the (111) terrace itself as a reference for all the other sites. We found two possible stable configurations for copper on the terrace, labeled C and D in Figs. 1 and 5. At site C, the copper atom effectively lies between two surface hydrogens and sits quite far from the silicon plane with a fairly small adsorption energy of −0.77 eV. Site D is clearly energetically favored, with the copper at the center of three hydrogens, but actually bonded to a silicon atom, increasing the adsorption energy to −1.17 eV.

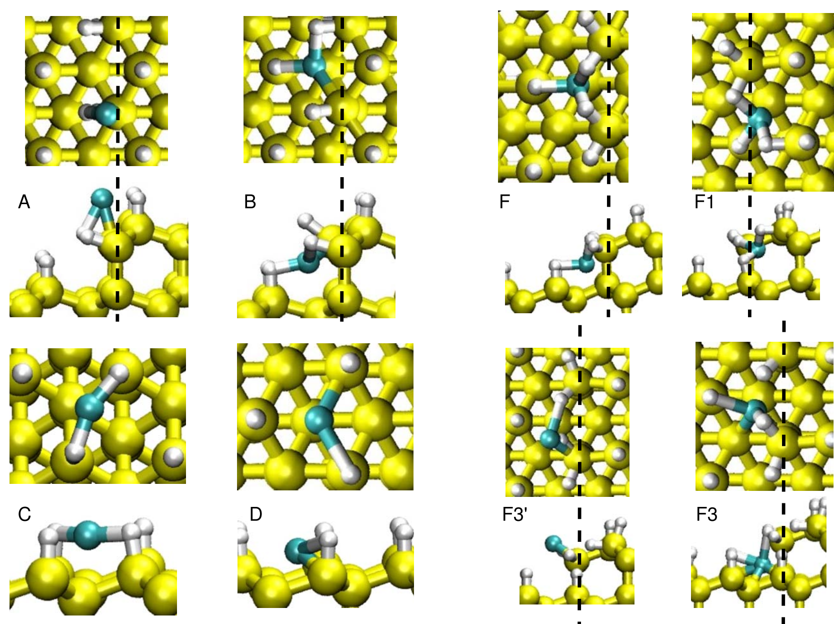

FIG. 5. (Color online) Overhead and side views of the atomic structure of copper adsorbed at different sites on the surface. Silicon is represented by large yellow (large light gray) spheres, copper by small blue (dark gray) spheres, and hydrogen by small white spheres.

At a monohydride step, we can consider adsorption either above (A) or below (B) the step edge (see Figs. 1 and 5). Above the step edge, the copper forms weak bonds with the silicon monohydride and has an adsorption energy of only −0.55 eV. Below the step edge, at site B, the bonding opportunities are increased, and we see a corresponding increase in energy to −0.89 eV. However, both these sites are energetically less favorable than adsorption at the D terrace site. We can also consider creating kink sites at this step edge by removing atoms, and investigating whether these sites are especially reactive. The kinks are created by removing Si-H groups from the step edge and then saturating all remaining dangling bonds with hydrogen. Initially, we removed a single monohydride (Si and H labeled 1 in Fig. 1) from the step edge and found that copper adsorbs weakly at this site with an energy of only −0.65 eV (M in Table I). Removing a second SiH from just behind the step edge (labeled 2 in Fig. 1) increases the bonding possibilities for copper. It sits at the original step edge site and bonds to four hydrogens, increasing the adsorption energy to −1.27 eV (N in Table I).

On the horizontal dihydride step, the presence of two hydrogens at the step edge increases the number of stable adsorption sites, and we find four possible sites (see Fig. 2). The least favorable site, G, is above the step next to the dihydride with an adsorption energy of −0.63 eV, bonding mainly with the hydrogen of the stable terrace silicon. The H site is the lowest energy site for copper above the step with an energy of −1.39 eV—larger than for terrace adsorption. This is because the copper effectively sits in a hollow between five silicons and a hydrogen from the step edge (the silicon seen at label H in Fig. 2 is actually in the lower layer). Below the step edge, we find a reasonably strong adsorption at site E (−1.01 eV), directly opposite and bonded to both hydrogens of a dihydride, but a much stronger adsorption is seen at site F (see Figs. 2 and 5). The adsorption energy of −1.43 eV is one of the highest on the surface, with copper clearly bonding to hydrogens from neighboring dihydrides and to a terrace hydrogen.

As for the monohydride step, we find only a single stable adsorption site above and below the vertical dihydride step. There is very weak adsorption above the step, and the only stable site (K in Fig. 3) is directly above the step dihydride with an adsorption energy of −0.50 eV. Below the step, at site J, this increases to −1.10 eV, following the trend for increased adsorption below the step edge.

In Fig. 4, we explicitly consider kinks in a horizontal dihydride step and a monohydride step. These kinks present several sites with a large density of terminating hydrogens and a corresponding reduction in silicon-silicon bonds near the adsorption site. As such, we would expect to obtain generally high adsorption energies at these sites due to the increased charge density available for bonding. In fact, site F1 [see Figs. 4(a) and 5] has the largest adsorption energy on the surface, −1.44 eV. The copper is *nested* in the kink hollow and forms bonds with the surrounding atoms. Out of the hollow, at site F3, the energy is reduced to −1.34 eV but still represents a strong adsorption site. In contrast, above the kink at site F3′, we find the lowest adsorption energy on the surface, −0.43 eV, emphasizing the importance of the proximity of potential bonding sites. For the kink on the monohydride step (see Fig. 4), we see the same behavior. The hollow at the kink is more favorable (site I), with an adsorption energy of −1.34 eV, comparable to the F sites at the dihydride kink. Site L outside the hollow has a less favorable adsorption energy of −1.01 eV due to a lower density of terminating hydrogens. Further kink sites have adsorption configurations very similar to those of sites A, G, and L (see Fig. 32 in Ref. 6).

2. Charge density analysis

The previous discussion of copper bonding was based on the visualization of the calculated geometry and, as such, is not a very accurate method for determining the real bonding of copper to the surface. In order to better understand the adsorption energy hierarchy, we also performed a detailed analysis of the electron density for each configuration.

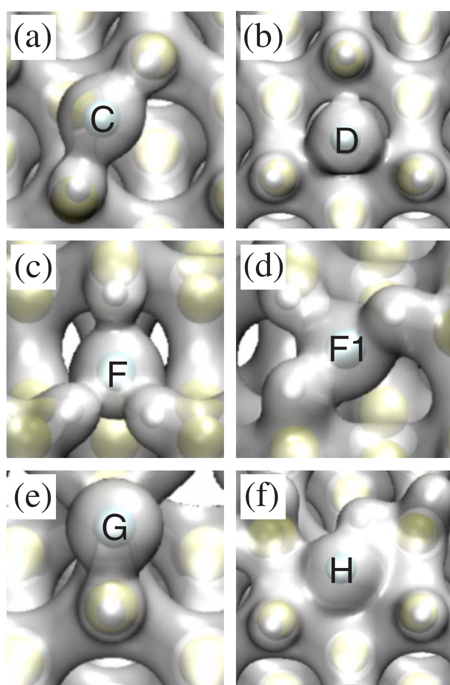

FIG. 6. (Color online) Electron densities for different copper adsorption sites plotted from above at an isosurface of 0.019 e/Å^3.

Figure 6 shows electron density plots for the cases which we will consider in detail.

On the terrace, there was a significant difference in energy between adsorption at site C and at site D (see Fig. 1), which we ascribed to the fact that at site D copper bonds to terrace silicon atoms. Figure 6 confirms this and shows that at C, copper bonds to two hydrogens, but at D, it bonds with all three silicon atoms surrounding it. An even larger difference in adsorption energy is found at sites G and H (see Fig. 2), despite their proximity on the surface. The difference is again due to the number of possible bonds—at G only a single strong bond is formed with a hydrogen, whereas at H the copper bonds significantly with five silicons and a hydrogen. As one would expect, the two most favorable sites on the surface, F and F1 (see Fig. 5), have very similar bonding configurations, forming strong bonds to two hydrogens above and one hydrogen below the step.

The nature of the bonding between copper and the surface can also be understood by looking into the details of the electronic configuration of the absorbed atom. The isolated atom has a ground state with a single 4s electron and ten 3d electrons, and is spin polarized. Adsorption sites on the surface with a low adsorption energy produce a similar electronic configuration. For example, copper at sites A and F3′ retains all its electrons and a spin polarized 4s orbital. In contrast, sites demonstrating strong adsorption, for example, F1 and F3, show a significant transfer of charge from the 4s orbital to the surface and are no longer spin polarized.

The adsorption energetics of all the other configurations on the surface can be understood in a similar way, with the density and character of available bonds determining the strength of adsorption. Although this seems an obvious conclusion, ongoing studies with other metal impurities show that copper is especially sensitive to the local environment at the adsorption site.

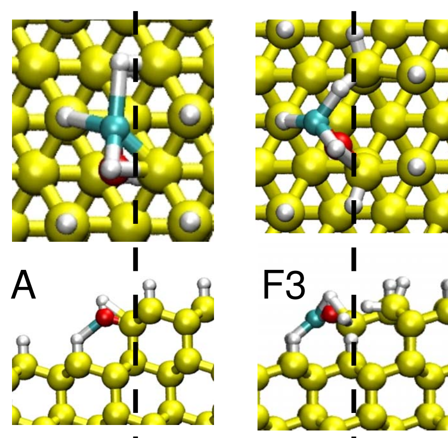

FIG. 7. (Color online) Overhead and side views of the atomic structure of copper adsorbed at OH-terminated A and F3 sites on the surface. Silicon is represented by large yellow (large light gray) spheres, copper by small blue (dark gray) spheres, hydrogen by small white spheres, and oxygen by the large red (black) spheres.

B. Adsorption on the partially OH-terminated surface

For the applications where water or etchants are present, it is also important to consider the role of hydroxyl groups on the surface. In order to study this, we calculated the adsorption of copper at several characteristic surface sites where a single hydrogen was replaced by an OH—these sites vary from a weak to a strong copper adsorption without OH and include terrace, step, and kink sites. Table I gives the energies for the six cases considered—for simplicity, we have kept the same labels as for the H-terminated sites even though the adsorption geometry can be quite different. For example, the relaxed configuration of site A with an OH present is closer to site B without an OH rather than A. In general, our calculations did not show a large variation in adsorption energies for the OH group itself, although we only considered the low density limit; hence, we focus only on how the presence of the OH group changes the adsorption probability for copper.

The first observation from the OH calculations is that although there is no uniform increase in copper adsorption energies for all sites, the average energy for similar sites has increased compared to the H-terminated case, from −1.05 to −1.18 eV. The spread of values has also reduced from 0.89 to 0.36 eV, suggesting that copper would be much more uniformly distributed in the presence of OH groups. This can be understood simply from the fact that copper has a stronger interaction with the oxygen of the OH group than with any surface species, and the adsorption is dominated by the accessibility of this oxygen. At site A, for hydrogen termination, we obtained a very small adsorption energy of −0.55 eV due to the isolation of the site from potential bonding sites. However, the isolation of an OH at this site allows copper to form a strong bond, dramatically increasing the adsorption energy to −1.38 eV (see Fig. 7). For similar rea-

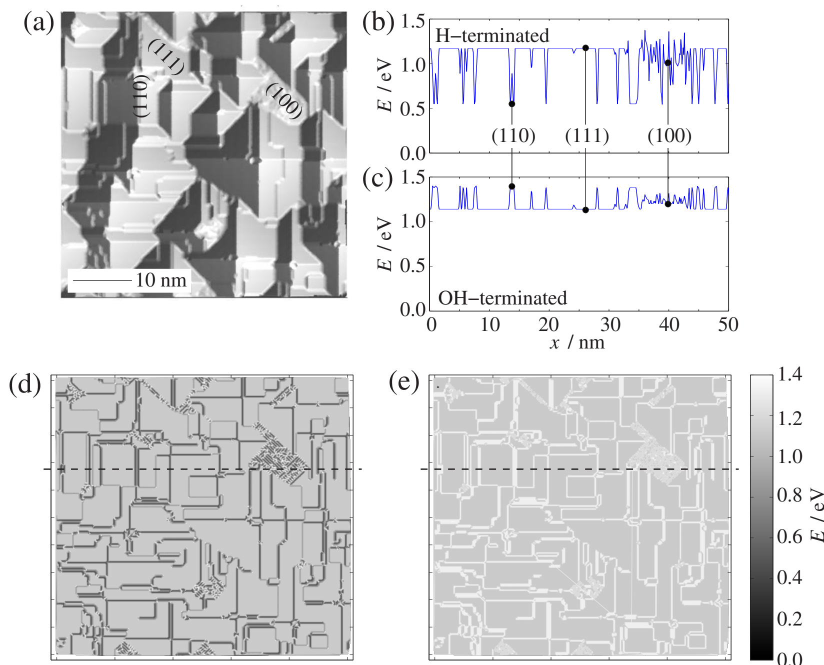

FIG. 8. (Color online) (a) Structure of a 50 $\times 50$ nm^2 etched (100) silicon surface, adsorption energy profiles for the (b) H-terminated and (c) OH-terminated surfaces, (d) plot of the copper adsorption energy across the surface for hydrogen termination, and (e) plot of the copper adsorption energy across the surface for hydroxyl termination. The dashed lines in (d) and (e) mark the path of the energy profiles.

sons, we also see increases in bonding at sites C and E. In contrast, at sites F1 and F3, where there was already a high density of potential bonding sites, the OH group effectively blocks some of these sites and the Cu-O bond does not provide enough compensation (compare F3 in Figs. 5 and 7). Site D lies in between these two extremes, and we see almost no change in the adsorption energy.

C. Visualization of the adsorption energy landscape

Now that we have calculated the energetics of copper adsorption on the surface, it is interesting to visualize the "adsorption field" on a realistic surface. Here, we have used a Monte Carlo simulation of anisotropic wet chemical etching[6,35,36] to reproduce the major morphologic features of the etched (100) surface of silicon at low concentration. Under these conditions, the experimental surfaces typically display pyramidal hillocks similar to those shown in Fig. 8(a), corresponding to 300 000 Monte Carlo steps of the simulation. Note that in order to produce a realistic rough surface and, hence, a wide variety of surface sites, the simulation includes the role of impurities in the etching process as micromasking (or pinning) centers. A general explanation of the role of impurities in anisotropic wet chemical etching based on experimental results and general theoretical micromasking arguments can be found in Ref. 6. A corresponding simulation methodology, which is beyond the scope of this paper, is under development to quantitatively link the experiments and the pinning effects. In the present work, the morphology of the surface in Fig. 8(a) acts as a useful demonstrative example of a real surface. It provides a realistic morphology for the visualization of the adsorption energy landscape for copper.

Although the surface is initially a crystallographic cut of (100), the anisotropy of the etching process, combined with the pinning of some dihydride sites, results in facets of (111) and (110) and a large number of step and kink sites. In order to plot the adsorption energies across the whole surface, we project the H and OHs on the surface onto a slightly tilted horizontal plane and produce a Delanauy triangulation[37] of the resulting two-dimensional point cloud using the Bowyer-Watson algorithm.[38,39] After this, we are able to identify each triangle with a copper adsorption site and assign colors to the triangles according to the calculated adsorption energies. Figure 8(d) shows the result of this visualization procedure for a hydrogen-terminated surface—an almost uniform energy isosurface across the (111) terraces, increased adsorption energy at dihydride steps and kinks (around the (100) facet), and low energy at monohydride steps at the edge of (111) terraces. In contrast, if we consider the extreme case of complete OH termination [see Fig. 8(e)], the energy map is much more uniform, with little difference between (111) terraces and step and kink sites. The differences between the two energy landscapes are highlighted in Figs. 8(b) and 8(c) by using cross sections.

We note that the link between the *ab initio* calculations and Monte Carlo (MC) simulations is not yet complete, and Fig. 8(e) should not be considered literally. Firstly, the *ab initio* calculations do not take into account the interaction between the hydroxyls, yet Fig. 8(d) assumes full OH coverage, completely disregarding those interactions. In reality, a varying percentage of the surface sites are expected to be hydroxyl terminated, depending on the etchant concentration. Figures 8(d) and 8(e) represent two extreme cases and suggest that the adsorption of copper can be rather different at low and high concentrations. Furthermore, the MC simulation in Fig. 8(a) is not coupled to the energy landscapes in Figs. 8(d) and 8(e). In the future, we would like to couple the surface evolution and the copper adsorption energies dynamically in order to understand whether copper can have a role as a micromasking agent during anisotropic etching. The previous energy landscape visualization represents an initial effort to fulfill this target.

IV. DISCUSSION

In general, we have shown that copper can adsorb strongly to the H-terminated silicon surface and that the adsorption energy is significantly dependent on the local bonding environment. Sites which offer several hydrogen or silicon bonds, such as dihydride steps and kinks, are most favorable, whereas exposed step or terrace sites are less favorable. The addition of a hydroxide group increases the average adsorption energy while reducing the range of adsorption energies. The strong interaction between copper and oxygen reduces the influence of the local bonding environment, and adsorption is more homogeneous.

It is interesting that our results completely contradict previous calculations[23] of the same system. These authors found adsorption energies of less than 0.1 eV on H-terminated sites and about 0.3 eV for OH-terminated sites (compared to over 1.0 eV in our calculations) using 11–14 atom cluster models. The huge difference in energies cannot be explained by any differences in exchange-correlation functional or basis set, so we performed an adsorption calculation using the method described in Sec. II A and their Si_4H_{10} monohydride cluster. We found a local minimum with an adsorption energy of 0.3 eV at a geometry similar to that presented in Ref. 23, but less symmetric. However, this was not the ground state in our calculations, and we found that copper prefers to sit just above the center of three silicons close to the central monohydride silicon. This has a larger adsorption energy of 0.5 eV. This agrees with the bonding trends seen in our results, that sites with more potential bonds are favored, but clearly a small cluster is insufficient to model the real surface accurately. The qualitative result reached in Ref. 23, that copper prefers to adsorb at dihydride rather than monohydride sites on the surface, agrees with our results and supports experiments studying copper nucleation.[40–44]

These calculations are part of a larger effort to include the role of metal impurities in a multiscale model of anisotropic wet chemical etching. Although a quantitative comparison with etching experiments still requires full integration of these results into mesoscale simulations, we can compare the general trends. Experimental studies of the role of metal impurities (studying the role of Ag, Al, Cr, Cu, Pb, Zn, Ni, Fe, and Mg) in etching[6,25,26] demonstrate that copper increases the surface roughness and reduces the etch rate, and, apart from lead, all other impurities have minimal effect. Lead also reduces the etch rate, but has no influence on the surface roughness. The effects of the copper impurities can be understood experimentally based on the idea of copper as a micromask, locally pinning or blocking sites. Our results predict that there is a clear preference for copper to adsorb at dihydride steps, and this would explain the changes in morphology seen experimentally. Furthermore, the experiments observe that as the concentration of etchant increases, the effect of the copper is changed due to an increase in the reactivity of monohydride steps, again corresponding to the theoretically predicted change in adsorption energies in the presence of OH groups. As a control, we also calculated the adsorption of lead and magnesium on the H-terminated surface, and found that magnesium does not adsorb at all and that lead adsorbs with a completely different adsorption energy hierarchy. The details of these studies will be published later.

ACKNOWLEDGMENTS

We acknowledge the generous computer resources from the Center for Scientific Computing, Helsinki, Finland. This research has been supported by the Academy of Finland through its Centers of Excellence Program (2006–2011) and Project No. SA 212603, by the Finnish Cultural Foundation (T. Hynninen), by the Japanese Center of Excellence Programme “Micro- and Nano-Mechatronics for Information-Based Society” (2003–2007) and the JSPS-Bilateral Program with the Academy of Finland.

*asf@fyslab.hut.fi; www.fyslab.hut.fi/~asf/physics

[1] M. Hourai, T. Naridomi, Y. Oka, K. Murakami, S. Sumita, N. Fujino, and T. Shiraiwa, Jpn. J. Appl. Phys., Part 2 **27**, L2361 (1988).
[2] T. Heisera, A. A. Istratov, C. Flink, and E. R. Weber, Mater. Sci. Eng., B **B58**, 149 (1999).
[3] A. A. Istratov and E. R. Weber, J. Electrochem. Soc. **149**, G21 (2002).
[4] W. Kern, J. Electrochem. Soc. **137**, 1887 (1990).
[5] O. M. R. Chyan, J. J. Chen, H. Y. Chien, J. Sees, and L. Hall, J. Electrochem. Soc. **143**, 92 (1996).
[6] M. A. Gosálvez, K. Sato, A. S. Foster, and R. M. Nieminen, J. Micromech. Microeng. **17**, S1 (2007).
[7] N. Tokuda, D. Hojo, S. Yamasaki, K. Miki, and K. Yamabe, Jpn. J. Appl. Phys., Part 2 **42**, L1210 (2003).
[8] N. Tokuda, H. Watanabe, D. Hojo, S. Yamasaki, K. Miki, and K. Yamabe, Appl. Surf. Sci. **237**, 529 (2004).
[9] N. Tokuda, M. Nishizawa, K. Miki, S. Yamasaki, R. Hasunuma, and K. Yamabe, Jpn. J. Appl. Phys., Part 2 **44**, L613 (2005).
[10] L. A. Baker, A. R. Laracuente, and L. J. Whitman, Phys. Rev. B **71**, 153302 (2005).
[11] J.-Z. Wang, J. F. Jia, X. Liu, W. D. Chen, and Q. K. Xue, Phys. Rev. B **65**, 235303 (2002).
[12] M. Hanbücken and G. L. Lay, Surf. Sci. **168**, 122 (1986).
[13] L. Barbier and J. Lapujoulade, J. Vac. Sci. Technol. A **8**, 2662 (1990).
[14] T. Ichinokawa, T. Inoue, H. Izumi, and Y. Sakai, Surf. Sci. **241**, 416 (1991).
[15] S. Guillet, L. E. Regalado, T. Lopez-Rios, and R. Cinti, Appl. Surf. Sci. **65/66**, 742 (1993).
[16] P. W. Murray, R. Lindsay, F. M. Leibsle, P. L. Wincott, and G. Thornton, Phys. Rev. B **54**, 13468 (1996).
[17] B. Z. Liu, M. V. Katkov, and J. Nogami, Surf. Sci. **453**, 137 (2000).
[18] S. K. Estreicher, Phys. Rev. B **60**, 5375 (1999).
[19] S. K. Estreicher, Mater. Sci. Semicond. Process. **7**, 101 (2004).

[20] C. D. Latham, M. Alatalo, R. M. Nieminen, R. Jones, S. Oberg, and P. R. Briddon, Phys. Rev. B **72**, 235205 (2005).
[21] F. J. H. Ehlers, A. P. Horsfield, and D. R. Bowler, Phys. Rev. B **73**, 165207 (2006).
[22] T. Yasue and T. Koshikawa, Surf. Sci. **377-379**, 923 (1997).
[23] K. Tatsumura, T. Watanabe, K. Hara, T. Hoshino, and I. Ohdomari, Phys. Rev. B **64**, 115406 (2001).
[24] H. Tanaka, Y. Abe, T. Yoneyama, J. Ishikawa, O. Takenaka, and K. Inoue, Sens. Actuators, A **A82**, 270 (2000).
[25] H. Tanaka, Y. Abe, K. Inoue, M. Shikida, and K. Sato, Sens. Mater. **15**, 43 (2003).
[26] H. Tanaka, Ph.D. thesis, Nagoya University, Japan, 2005.
[27] G. S. Higashi, Y. J. Chabal, G. W. Trucks, and K. Raghavachari, Appl. Phys. Lett. **56**, 656 (1990).
[28] M. A. Hines, Annu. Rev. Phys. Chem. **54**, 29 (2003).
[29] P. Allongue, Phys. Rev. Lett. **77**, 1986 (1996).
[30] J. Junquera, O. Paz, D. Sánchez-Portal, and E. Artacho, Phys. Rev. B **64**, 235111 (2001).
[31] J. M. Soler, E. Artacho, J. D. Gale, A. García, J. Junquera, P. Ordejón, and D. Sánchez-Portal, J. Phys.: Condens. Matter **14**, 2745 (2002).
[32] J. P. Perdew, K. Burke, and M. Ernzerhof, Phys. Rev. Lett. **77**, 3865 (1996).
[33] H. J. Monkhorst and J. D. Pack, Phys. Rev. B **13**, 5188 (1976).
[34] S. F. Boys and F. Bernadi, Mol. Phys. **19**, 553 (1970).
[35] M. A. Gosálvez, A. S. Foster, and R. M. Nieminen, Europhys. Lett. **60**, 467 (2002).
[36] M. A. Gosálvez, A. S. Foster, and R. M. Nieminen, Appl. Surf. Sci. **202**, 160 (2002).
[37] B. Delanauy, Otdelenie Matematicheskikh i Estestvennykh Nauk **7**, 793 (1934).
[38] A. Bowyer, Comput. J. **24**, 162 (1981).
[39] D. F. Watson, Comput. J. **24**, 167 (1981).
[40] K. Hara and I. Ohdomari, Jpn. J. Appl. Phys., Part 2 **37**, L1333 (1998).
[41] T. Homma, C. P. Wade, and C. E. D. Chidsey, J. Phys. Chem. B **102**, 7919 (1998).
[42] K. Hara, T. Tanii, and I. Ohdomari, Jpn. J. Appl. Phys., Part 1 **38**, 6860 (1999).
[43] K. Hara and I. Ohdomari, Appl. Surf. Sci. **144-145**, 476 (1999).
[44] S. W. Lim, R. T. Mo, P. A. Pianetta, and C. E. D. Chidsey, J. Electrochem. Soc. **148**, C16 (2001).